Hepatic progenitor cells reprogrammed from mouse fibroblasts repopulate hepatocytes in Wilson's disease mice

Kai Liu[1,2]*, Li Li[3,4], Yu He[3,4], Song Zhang[2], Hong You[3,4]* and Ping Wang[3,4]*

Abstract

Background Wilson's disease (WD) is a genetic disorder that impairs the excretion of copper in hepatocytes and results in excessive copper deposition in multiple organs. The replacement of disordered hepatocytes with functional hepatocytes can serve as a lifelong therapeutic strategy for the treatment of WD. The aim of this study was to determine the hepatocyte repopulation effects of fibroblast-derived hepatic progenitor cells in the treatment of WD.

Methods Induced hepatic progenitor cells (iHPCs) were generated through direct reprogramming of adult mouse fibroblasts infected with lentivirus carrying both the *Foxa3* and *Hnf4a* genes. These iHPCs were subsequently identified and transplanted into copper-overload WD mice with the *Atp7b* (H1071Q) mutation *via* caudal vein injection.

Results After lentivirus infection, the fibroblasts transformed into *Foxa3*- and *Hnf4a*-overexpressing cobblestone-like cells with reduced expression of fibroblast markers and increased expression of epithelial cell and hepatic progenitor cell markers, i.e., iHPCs. Sixteen weeks after transplantation into WD mice, approximately 2% of hepatocytes were derived from iHPCs, and these iHPC-derived hepatocytes expressed a tight junction-associated protein of the bile canal, tight junction protein 1 (Zo1). There was a decrease in the serum copper concentration and relative activity of serum ceruloplasmin at weeks 4 and 8 after iHPCs transplantation compared with those of WD fed mice administered saline or fibroblasts. Furthermore, iHPC transplantation markedly reduced the proportion of CD8^{+} T lymphocytes and natural killer cells compared with those in fibroblast-transplanted WD mice and downregulated the transcription of the inflammatory cytokines, including tumor necrosis factor α (*Tnfa*), interleukin 1β (*IL-1β*), and *IL-6*, compared with those in WD mice and in fibroblast-transplanted WD mice.

Conclusion iHPCs reprogrammed from adult fibroblasts can repopulate hepatocytes and exert therapeutic effects in WD mice, representing a potential replacement therapy for clinical application.

*Correspondence:
Kai Liu
lkfriendship@qq.com
Hong You
youhongliver@ccmu.edu.cn
Ping Wang
wangping2009@ccmu.edu.cn
Full list of author information is available at the end of the article

Highlights

- Simultaneous overexpression of Foxa3 and Hnf4α can reprogram fibroblasts into homogenous hepatic progenitor cells.
- After transplantation, these reprogrammed hepatic progenitor cells integrate into liver tissue and participate in liver copper excretion and serum copper reduction in WD mice.
- Compared with those in fibroblast-transplanted WD mice, transplantation of these reprogrammed hepatic progenitor cells markedly reduced the proportions of CD8^{+} T lymphocytes and natural killer cells and downregulated the transcription of the inflammatory cytokines *Tnfa*, *IL-1β*, and *IL-6*.

Keywords Wilson's disease, Induced hepatic progenitor cells, Foxa3, Hnf4α

Graphical Abstract
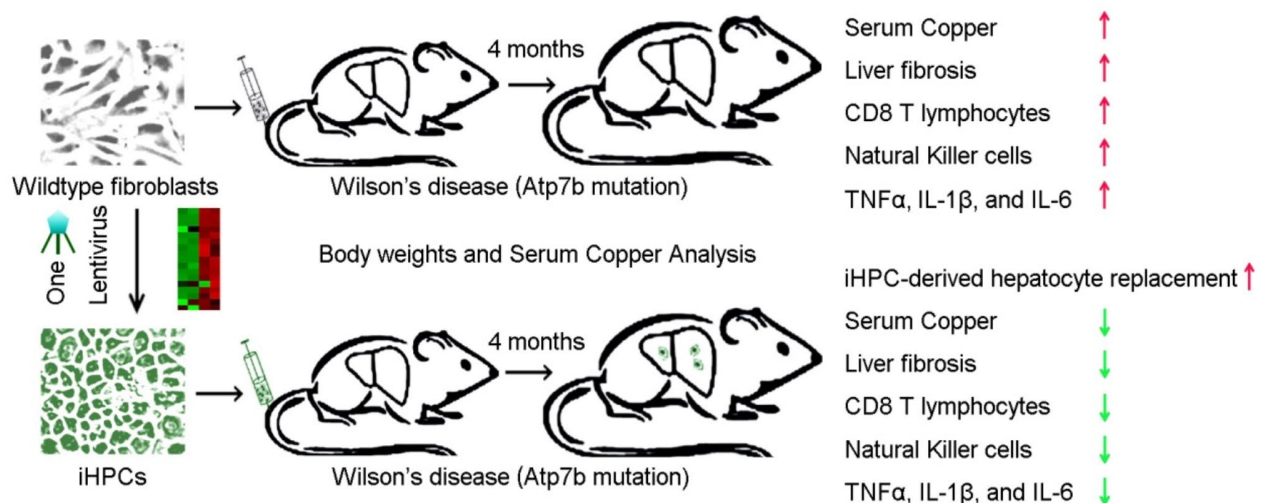
Introduction

Wilson's disease (WD) is a rare autosomal recessive disease with an estimated prevalence of 1 in 30,000 inhabitants and a one-allele mutation carrier frequency of 1 in 90 [1]. WD arises from homozygous or compound heterozygous mutations in the *ATP7B* gene, which leads to dysfunction of the transmembrane copper-transporting P-type adenosine triphosphatase (ATPase), thus reducing copper excretion into the bile [1, 2]. Copper overload in hepatocytes and excess copper leakage into the circulation result in excessive copper deposition in the liver and extrahepatic organs, which increases oxidative stress, impairs cell functions, and eventually leads to cell death. The currently available WD management options are life-long pharmacological therapies or orthotopic liver transplantation. Pharmacological treatments for WD, such as chelators and zinc salts, are generally effective for patients if used throughout their lifetime. However, approximately one-third of patients have drug-induced side effects, up to half of neurologically affected patients experience worsened neurological symptoms, and approximately one-quarter of patients cannot adhere to anti-copper regimens because of adverse effects and/or complex treatment [3]. Although liver transplantation is curative for WD and patients recover from WD syndrome after liver transplantation, organ scarcity greatly limits its application [4]. Therefore, new therapeutic strategies for WD are urgently needed.

As liver transplantation can correct defects in hepatocyte copper excretion, the transplantation of healthy hepatocytes with normal copper-transporting P-type ATPases has curative effects on WD. Although transplantation of mature hepatocytes rescues rats with Wilson's disease from fulminant hepatitis [5, 6], the difficulties in expanding hepatocytes and maintaining their functions in vitro make hepatocyte transplantation reliant on donor livers. The ability to convert somatic fibroblasts into expandable hepatocyte-like cells [7–10] or bipotential hepatic stem-like cells [11] *via* the ectopic expression of liver-enriched transcription factors, notably the pioneer transcription factor forkhead box *a1/2/3* (*Foxa1/2/3*) and the hepatocyte differentiation-initiating transcription factor hepatocyte nuclear factor *1α/4α* (*Hnf 1α/4α*), provides new possibilities for generating hepatocytes, which rescue mice from foetal fumarylacetoacetate hydrolase (Fah) deficiency or concanavalin A/carbon tetrachloride-induced acute liver injury. However, these reprogramming protocols involve the overexpression of

multiple liver-enriched transcription factors *via* multiple individual viral vectors, thus resulting in a heterogeneous cell population with different conversion efficiencies [12]. Although constructing multiple genes in one polycistronic vector could simultaneously convey ectopic liver-enriched transcription factors for reprogramming fibroblasts [13–16], the expression of the ectopic genes may decrease if they are designed towards the end of the vector, and the protein functionality of the ectopic genes may also be affected by N- or C-terminal fusion [17]. Therefore, multigene coexpression by different promoters may be a better strategy for preserving ectopic gene function in fibroblast reprogramming.

Considering the different mixtures of liver-enriched transcription factors used to reprogram murine or human fibroblasts, two core reprogramming factors, *Foxa3* and *Hnf4α*, are commonly used, especially for multiple genes in one polycistronic vector [13–16]. Therefore, in this study, a single viral vector containing *Foxa3* and *Hnf4α* with their own promoters was used to reprogram mouse adult fibroblasts into homogenous expandable hepatic progenitor-like cells. Considering that few studies have used these fibroblast-reprogrammed hepatocyte-like cells or stem/progenitor-like cells to treat mice with inherited metabolic disorders, including WD, for hepatocyte repopulation, these cells were transplanted into *Atp7b* (H1071Q) point mutation WD mice. These reprogrammed cells could be incorporated into liver tissue and differentiate into mature hepatocytes to reduce copper concentrations and relieve liver inflammation and collagen deposition, thus providing a new cell therapy strategy for WD.

Materials and methods

Ethics statement

All experiments involving animals were conducted in accordance with the ethical policies and procedures approved by the Ethics Committee of Beijing Friendship Hospital, Capital Medical University, China (Approval No. 21-2051). The title of the approved project is "Study on the Mechanism of iHPCs Therapy in Wilson's Disease." The approval date is December 30, 2021. All mice were performed during and at the end of the experiment under sodium pentobarbital anaesthesia, and animals were sacrificed using CO2 inhalation. The work has been reported in line with the ARRIVE guidelines 2.0. Every effort was made to minimize animal suffering.

Mice

The mice utilized in this study were all male, weight-matched, randomly assigned, and approximately eight weeks old. Wild-type C57BL/6J mice were purchased from Beijing Vital River Laboratory (Beijing, China). Heterozygous *Atp7b*(H1071Q) point mutation WD mice

with a genetic background of C57BL/6J were purchased from Shanghai Model Organisms (Shanghai, China). The mice were housed under specific pathogen-free mouse facilities at Beijing Friendship Hospital.

Foxa3 and *Hnf4α* overexpression lentivirus production

A lentiviral vector, pHS-B-0164, was constructed to carry full-length *Foxa3* (mouse, NM_008260) with a triplicate Flag (3XFlag) and full-length *Hnf4α* (mouse, NM_008261) under the control of the EF1α promoter and CMV promoter, respectively. This vector was cotransfected into 293T cells together with the packaging plasmids psPAX2 and pMD2.G to produce the lentivirus (Beijing Syngentech Corporation, Beijing, China).

Adult fibroblast primary culture and iHPC induction

Ears from two 2-month-old wild-type C57BL/6J mice were cut in a sterile environment and minced into small pieces, followed by digestion with 0.01% trypsin (Gibco, Grand Island, NY) and 0.1% type IV collagenase (Sigma−Aldrich, Saint Louis, MO) for 120 min at 37 °C. After filtration through a 100 μm cell strainer and washing with phosphate-buffered saline (PBS), the cells were plated on 0.1% gelatine (Sigma−Aldrich)-coated dishes in DMEM (Stemcell, Vancouver, Canada) containing 10% foetal bovine serum (FBS, Gibco). After 7 days of culture, the fibroblasts were digested and transferred into new dishes at passage 1, and the fibroblasts at passages 2 and 3 were used for induced hepatic progenitor cell (iHPC) induction.

For iHPC induction, fibroblasts were infected with lentivirus containing an empty vector or a vector containing *Foxa3* and *Hnf4α*. After 24 h of infection, the medium was replaced with DMEM/F12 (Stemcell) supplemented with 10% FBS, 1×ITS (Sigma−Aldrich), 20 ng/mL hepatocyte growth factor (HGF, Peprotech, Rocky Hill, CT) and 10 ng/mL epidermal growth factor (EGF, Peprotech). After 14 days of culture, colonies of iHPCs were removed and passaged continuously.

Indirect immune cytochemistry

The iHPCs and the empty vector control cells growing on the slides were fixed with 4% paraformaldehyde (PFA, Sigma−Aldrich). After permeabilization with 0.1% Triton X-100 (Sigma−Aldrich) and blocking with 3% bovine serum albumin (BSA, Sigma−Aldrich) in PBS, the cells were incubated with primary antibodies, including anti-Flag antibodies (Biolegend, San Diego, CA) and anti-Zo1 antibodies (Servicebio, Wuhan, China), at 4 °C for 60 min. After 3 washes with PBS, the cells were further incubated with secondary antibodies, including Alexa488-labelled goat anti-rat IgG (Servicebio) and Cy3-labelled goat anti-rabbit IgG (Servicebio), at 4 °C for 30 min. After 3 washes with PBS, the cells were observed under a Nikon Eclipse

fluorescence microscope (Nikon Corporation, Otahara, Japan) or acquired on a BD FACS Calibur flow cytometer (Becton Dickinson, Franklin Lakes, NJ). The FACS data were analysed *via* FlowJo software (Treestar, Ashland, OR).

Real-time PCR

Total RNA from 1×10^6 cells was extracted *via* an RNeasy mini-kit (Qiagen, Valencia, CA) according to the manufacturer's instructions. The RNA was reverse transcribed into cDNA *via* a SuperScript RT-kit (Invitrogen, Carlsbad, CA). Quantitative PCR analyses were carried out with triplicate samples of cDNA on an ABI 7500 Fast Real-time PCR system (Applied Biosystems, Foster City, CA) with SYBR Green PCR Mix (Applied Biosystems). The expression levels of each gene were normalized to Gapdh *via* the $2^{-\Delta\Delta Ct}$ method. The primers used are listed in Supplementary Table 1.

Western blot analysis

Total protein from 1×10^6 cells was extracted, and a standard western blot procedure was performed. Briefly, after protein quantification with a BCA protein assay kit (Thermo, Waltham, MA), the protein samples (20 μg) were electrophoresed on 10% SDS polyacrylamide gels and transferred to a PVDF membrane (Millipore, Boston, MA). After being blocked with TBST buffer containing 5% nonfat dry milk, the membranes were incubated with one of the following primary antibodies: Hnf4α (Cell Signaling Technology, Danvers, MA, 1:1000), albumin (Alb, R&D Systems, Minneapolis, MN, 1:1000), E-cadherin (Cdh1, Abcam, Cambridge, UK, 1:1000), Foxa3 (Abcam, 1:1000), or β-Actin (Abcam, 1:1000). After being washed and incubated with horseradish peroxidase-conjugated anti-rabbit/mouse IgG antibodies (GE Healthcare, Chicago, IL, 1:5000), the proteins were visualized with enhanced chemiluminescence reagents (Millipore). Bands were detected with an automatic chemiluminescence imaging analysis system (Tanon, Shanghai, China).

Detection of glycogen

A periodic acid Schiff (PAS) assay (Sigma−Aldrich) was used to determine the presence of glycogen in the cells according to the manufacturer's instructions. Briefly, the cells growing on the slides were fixed with 95% ethanol at room temperature for 1 min. After 3 washes with tap water, they were oxidized with 1% periodic acid for 30 min and then incubated with Schiff's reagent for 30 min. After rinsing with tap water for 2 min, the slides were observed under a Leica Dmi1 light microscope (Leica Corporation, Heidelberg, Germany).

RNA sequencing analysis

All the experiments were performed and analysed by Biomarker Technologies Corporation (Beijing, China). Briefly, RNA integrity was assessed *via* the RNA Nano 6000 Assay Kit of the Agilent Bioanalyzer 2100 system (Agilent Technologies, Santa Clara, CA). The sequencing libraries were generated *via* the NEBNext UltraTM RNA Library Prep Kit for Illumina (NEB, Atlanta, GA) following the manufacturer's recommendations. Clustering and library preparations were sequenced on an Illumina platform, and paired-end reads were generated. The raw reads and further analysis were processed with a bioinformatic pipeline tool (BMKCloud online platform, www.biocloud.net). The resulting *P* values were adjusted *via* Benjamini and Hochberg's approach for controlling the false discovery rate. Genes with an adjusted *P* value < 0.01 according to DESeq2 were considered differentially expressed. The raw sequence data reported in this paper have been deposited in the Genome Sequence Archive with the accession number CRA010018 (https://ngdc.ncb.ac.cn/search/?dbId=gsa%26q=CRA010018).

iHPC transplantation into WD model mice

The male mice obtained from breeding the heterozygous *Atp7b*(H1071Q) point mutation WD mice were divided into five groups: wild-type control group ($N = 6$), wild-type control with dietary copper loading group ($N = 6$), saline-injection homozygous WD mice with dietary copper loading group ($N = 6$), fibroblast-transplanted homozygous WD mice with dietary copper loading group ($N = 6$), and iHPC-transplanted homozygous WD mice with dietary copper loading group ($N = 8$). Dietary copper was given when the mice were 8 weeks old *via* the drinking water with 0.03% copper acetate (Merck, Darmstadt, Germany), and the supplementation was continued until the end of the study [18]. Saline, fibroblasts (1×10^6/mouse) or iHPCs (1×10^6/mouse) were given by caudal vein injection at week 10. The body weights were recorded, and the caudal vein sera were collected every 4 weeks from 10-week-old to 26-week-old mice.

Isolation of hepatocytes and liver nonparenchymal cells

After mice were anesthetized, each mouse was perfused with 30 mL of PBS through the left ventricle to remove circulating blood cells in the liver. Then, the livers were carefully removed and digested with 0.01% type IV collagenase in Hanks' balanced salt solution (HBSS) for 30 min at 37 °C. The tissues were dissociated *via* a gentle-MACS dissociator (Miltenyi, Bergisch-Gladbach, Germany) and filtered through 70 μm strainers. The cell suspension was centrifuged at 50 × g for 5 min, and the cell pellets were washed twice with PBS as the mixture of liver parenchymal cells. The supernatant was centrifuged at 2000 rpm for 5 min, and the cell pellet was

resuspended in 30% Percoll (GE, Chicago, IL) in HBSS for centrifugation at 800 × g for 25 min. The cell pellets were washed twice with PBS as the mixture of liver non-parenchymal cells.

Next, for surface marker staining, the nonparenchymal cells were incubated with TruStain fcX™ (BioLegend) for 5 min on ice to block nonspecific staining, after which the cells were stained with antibodies from Biolegend. One group included FITC-labelled anti-mouse CD4 (BioLegend), PE-labelled anti-mouse CD3 (BioLegend), PerCP-labelled anti-mouse CD45 (BioLegend), and APC-labelled anti-mouse CD8a (BioLegend) antibodies. The second group included FITC-labelled anti-mouse CD3 (BioLegend), PE-labelled anti-mouse NK-1.1 (BioLegend), and APC-labelled anti-mouse F4/80 (BioLegend) antibodies. The third group included FITC-labelled anti-mouse CD11c (BioLegend), PE-labelled anti-mouse/human CD11b (BioLegend), and APC-labelled anti-mouse GR-1 (BioLegend).

For intracellular staining, the parenchymal cells were fixed with fixation buffer (BioLegend) and permeabilized with Perm Buffer (BioLegend). After being blocked with 3% BSA in PBS, the cells were incubated with Alexa488-labelled anti-Flag antibody (BioLegend) at 4 ℃ for 30 min. All samples were acquired on a BD FACS Calibur flow cytometer (BD), and the data were analysed *via* FlowJo software (TreeStar).

Liver section Immunofluorescence staining
The liver tissues were fixed in 4% paraformaldehyde and embedded in paraffin. The paraffin-embedded liver sections were subjected to standard immunofluorescence staining as described previously [19]. After deparaffinization, rehydration, and antigen retrieval, the liver sections were blocked with 3% BSA in PBS and incubated with anti-Flag antibody (BioLegend) and anti-Zo1 antibody (Servicebio) at 4 ℃ overnight. After three washes with PBS, the slides were incubated with Alexa488-labelled goat anti-rat IgG (Servicebio) and Cy3-labelled goat anti-rabbit IgG secondary antibodies (Servicebio) for 60 min in the dark. After three washes with PBS, the nuclei were stained with DAPI (Servicebio). Liver sections were examined *via* a Nikon Eclipse microscope (Nikon Corporation, Otahara, Japan).

Serum copper and ceruloplasmin measurement
The levels of serum copper were analysed with a copper assay kit according to the manufacturer's instructions (Nanjing Jiancheng Bioengineering Institute, Nanjing, China). The levels of ceruloplasmin were analysed with a ceruloplasmin assay kit according to the manufacturer's instructions (Nanjing Jiancheng Bioengineering Institute). After spectrophotometry analysis (Spectramax M3, Sunnyvale, CA, USA), copper levels were calculated *via* a

standard curve, and ceruloplasmin levels were presented as relative activity.

Histological analysis
Paraffin-embedded tissues were sectioned and stained with haematoxylin–eosin (HE) for routine pathologic examination or with Sirius red for visualization of the extracellular matrix or with Timm's sulfide silver method to detect copper deposition. The slices were scanned with a Leica Dmi1 (Leica Corporation, Heidelberg, Germany).

Statistics
The data were analysed with GraphPad Prism 6 software (version 6.02) and are presented as the means ± standard deviations (SDs). One-way ANOVA with Tukey's post hoc test was used for multiple comparisons; a two-tailed, unpaired t test was used for unmatched pairwise sample comparisons. Significant differences were defined as * for $P < 0.05$, ** for $P < 0.01$, *** for $P < 0.001$, and **** for $P < 0.0001$.

Results

Generation of iHPCs by reprogramming mouse fibroblasts *via Foxa3* and *Hnf4α* overexpression
To obtain a single viral vector carrying two liver-enriched transcription factors, mouse *Foxa3* with 3XFlag (tag: DYKDDDDK) and *Hnf4α* were cloned and inserted into the pHS-B-0164 lentiviral vector (Fig. 1A) and packaged into a lentivirus. After infection with lentivirus carrying *Foxa3* and *Hnf4α*, the fibroblasts transformed from spindle-shaped cells into typical epithelial cobble-stone-shaped iHPCs (Fig. 1B). Indirect immune fluorescence staining revealed that the control virus-infected fibroblasts were negative for Flag, whereas iHPCs were positive for Flag (Fig. 1C), and flow cytometry analysis revealed that the percentage of positive Flags was nearly 60% in iHPCs (Fig. 1D). Real-time PCR analysis revealed that the expression levels of *Foxa3* and *Hnf4α* in iHPCs were approximately 40-fold and 12-fold greater than those in fibroblasts and control virus-infected fibroblasts, respectively (Fig. 1E). Western blotting further confirmed the increased expression of Foxa3, Hnf4α, Alb, and Cdh1 in iHPCs (Fig. 1F). Giemsa staining revealed the epithelial morphology of iHPCs, in contrast to the morphology of control virus-infected fibroblasts, and PAS staining revealed the glycogen content within iHPCs (Fig. 1G). In addition, the reprogrammed cells could be successfully cryopreserved and serially passaged for more than 10 generations, whereas the control fibroblasts could not be passaged for more than 5 generations (Fig. 1G).

Gene expression profiles of iHPCs
To further explore the gene expression profiles of iHPCs, whole mRNA transcript analysis was performed to
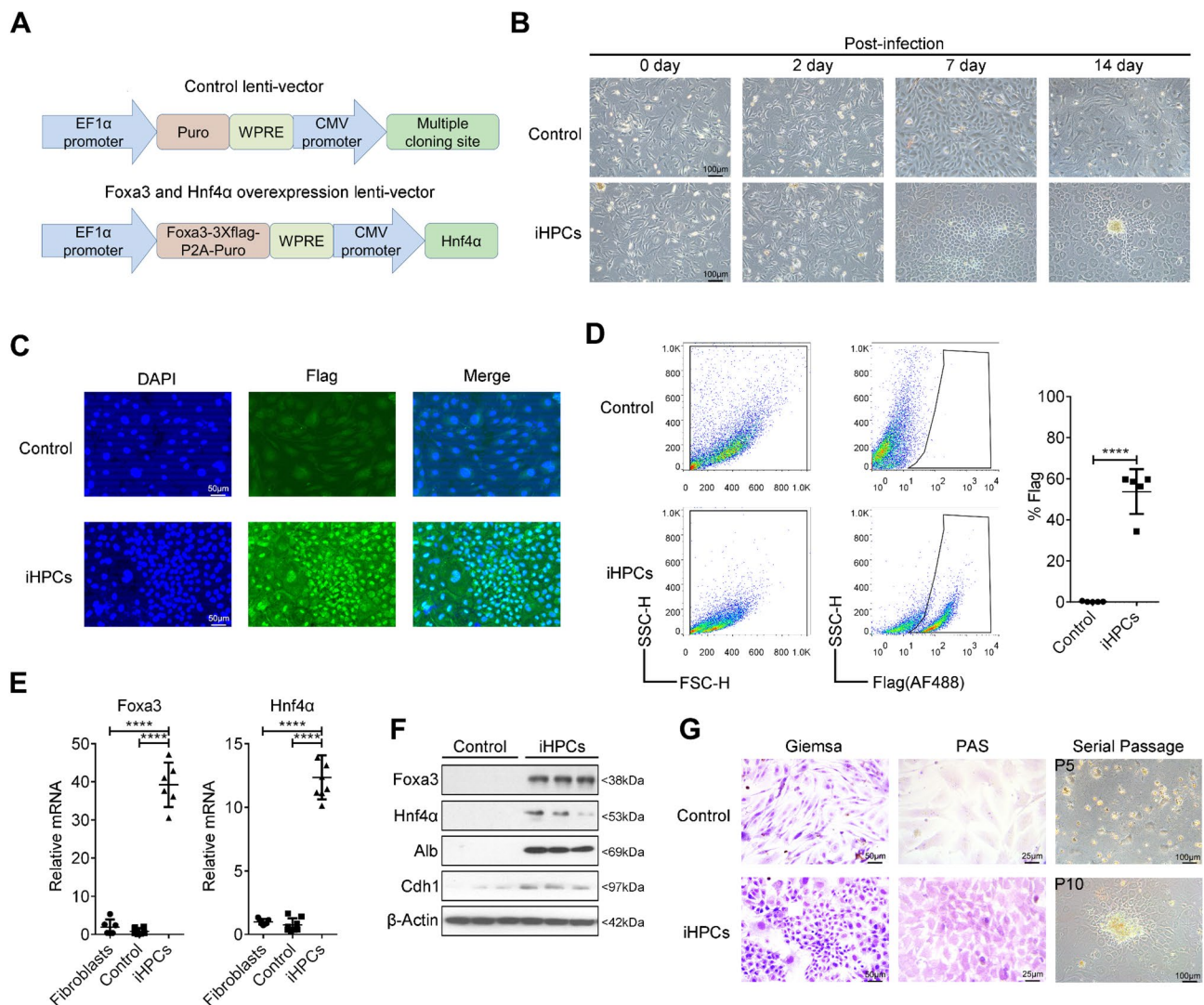
Fig. 1 Coexpression of *Foxa3* and *Hnf4a* reprogrammed mouse fibroblasts into iHPCs. **(A)** Constructs of the control-lentiviral vector and the overexpression-lentiviral vector carrying EF1α-promoter-driven *Foxa3* and CMV-promoter-driven *Hnf4α*. **(B)** Representative phase-contrast morphology of control fibroblasts and iHPCs on Days 0, 2, 7, and 14 after lentivirus infection. Scale bars, 100 μm. **(C)** Immunofluorescence staining Flag and DAPI in control fibroblasts and iHPCs. Scale bars, 50 μm. **(D)** Immunofluorescence staining and flow cytometry were used to analyse the percentages of Flag-positive control fibroblasts and iHPCs. **(E)** Real-time PCR was used to determine the relative expression of *Foxa3* and *Hnf4α* in control fibroblasts and iHPCs. **(F)** Western blot analysis showing the relative protein levels of Foxa3, Hnf4α, Alb, Cdh1, and β-Actin in control fibroblasts and iHPCs. β-Actin served as a loading control. **(G)** Giemsa staining (scale bars, 50 μm), PAS staining (scale bars, 25 μm), and phase-contrast morphology of control fibroblasts and iHPCs at serial passages (scale bars, 100 μm)

analyse the differences between iHPCs and control virus-infected fibroblasts or liver tissues. After quantification of gene expression and differential expression analysis, hierarchical clustering demonstrated that iHPCs were more similar to mouse liver tissues than control virus-infected fibroblasts (Fig. 2A). Moreover, iHPCs mimicked the gene expression profile of hepatocyte progenitor cells, including the upregulation of biomarkers involved in pluripotent stem cells (such as *Sox2*, *Tbx3*, and *Myc*), hepatoblasts (such as *Gata4*, *Gata6*, *Foxa*, and *Hnf*), proliferation (such as *Ki67*), and epithelial cells (such as *Cdh1*, *Zo1, and Zo2*) (Fig. 2B). Moreover, biomarkers for

fibroblasts and mesenchymal cells (such as *N-cadherin*, *Vimentin*, *Zeb*, and *Twist*) were downregulated in iHPCs (Fig. 2B). Moreover, real-time PCR analysis revealed a notable 4-fold increase in the expression of the progenitor cell marker *Sox9*, accompanied by an approximately 2-fold increase in the expression of the proliferation indicator *Ki67*. Additionally, there was a comparable 2-fold increase in the expression levels of hallmark hepatocyte markers, including *Alb*, *Cdh1*, and *Zo1*, in iHPCs compared with control virus-infected fibroblasts (Fig. 2C). The results obtained from immunofluorescence staining of *Zo1* (Fig. 2D) and the western blot analysis of
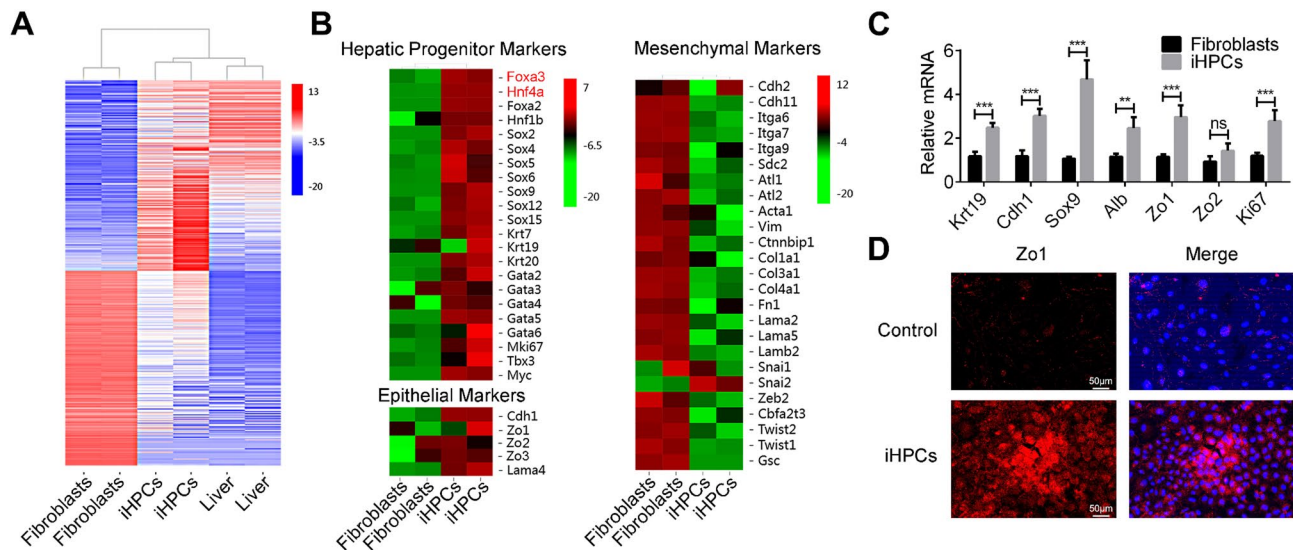
Fig. 2 iHPCs expressed a series of genes akin to those expressed by hepatocyte progenitor cells. **(A)** Transcriptome sequencing and hierarchical clustering analysis revealed differences between iHPCs and fibroblasts, as well as similarities between iHPCs and mouse liver tissues. **(B)** Comparison of the expression of markers of hepatic progenitor cells, epithelial cells and mesenchymal cells between iHPCs and fibroblasts via transcriptome sequencing data. **(C)** Real-time PCR confirmed the relative expression of *Krt19*, *Cdh1*, *Sox9*, *Alb*, *Zo1*, and *Ki67* in fibroblasts and iHPCs. **(D)** Representative images of immunofluorescence staining for Zo1 in control fibroblasts and iHPCs. Scale bars, 50 μm

Hnf4α, Alb and Cdh1 (Fig. 1F) were consistent with those derived from RNA detection. Therefore, the gene expression profiles of fibroblast-reprogrammed cells with relatively high expression of progenitor markers and proliferation markers but relatively low expression of mesenchymal markers suggest their phenotype of hepatic progenitor cells.

iHPC transplantation into the liver tissue of WD mice and differentiation into hepatocytes

To investigate the effects of iHPC transplantation on WD mice, iHPCs or control fibroblasts were transplanted into WD mice fed 0.03% copper acetate (Fig. 3A). There was no significant change in body weight among the groups after cell transplantation (Fig. 3B). At week 16 posttransplantation, there was no significant difference in organ morphology or signs of tumours in the liver or spleen (Fig. 3C). Neither the liver weights nor the spleen weights were significantly different (Fig. 3D and E).

Integration into liver tissue and differentiation into hepatocytes are essential for iHPC replacement of the defective hepatocytes in WD mice. To examine the integration and differentiation of iHPCs, liver cells from each mouse were isolated at week 16 posttransplantation. Intracellular staining and flow cytometry analysis revealed that approximately 2% of liver cells in iHPC-transplanted mice were Flag positive, which was significantly greater than those in the other groups ($P < 0.001$, Fig. 4A). Furthermore, these Flag-positive cells were detected by immunofluorescence in liver sections from iHPC-transplanted mice, whereas no Flag-positive

signals were detected in the other groups (Fig. 4B). In addition, these Flag-positive hepatocytes coexpressed Zo1 and were involved in tight junction formation between the Flag-positive transplanted hepatocytes and the Flag-negative recipient hepatocytes (Fig. 4C), suggesting the reconstitution of linear bile canaliculi.

iHPC transplantation ameliorated copper accumulation, collagen deposition, and inflammation

To investigate whether iHPC transplantation has therapeutic effects on copper accumulation in WD mice, the copper concentration and relative levels of ceruloplasmin in the serum were assayed at 0, 4, 8, 12, and 16 weeks after iHPC or fibroblast transplantation. Compared with those in wild-type mice fed copper acetate, the levels of serum copper significantly increased in copper acetate-fed WD mice and WD mice transplanted with control fibroblasts (Fig. 5A). However, at weeks 10, 14 and 18, the serum copper levels were markedly lower in the copper-overload WD mice transplanted with iHPCs than in the copper-overload WD mice transplanted with control fibroblasts, yet the difference was not significant at weeks 22 and 26 (Fig. 5A). Furthermore, the relative activities of serum ceruloplasmin were significantly lower in iHPC-transplanted WD mice than in saline-injected WD mice and WD mice transplanted with control fibroblasts at 4, 8, and 12 weeks posttransplantation (Fig. 5B). In addition, copper overload slightly increased immune cell infiltration, extracellular matrix deposition, and copper accumulation in the liver tissues of WD mice compared with those of wild-type mice with or without copper
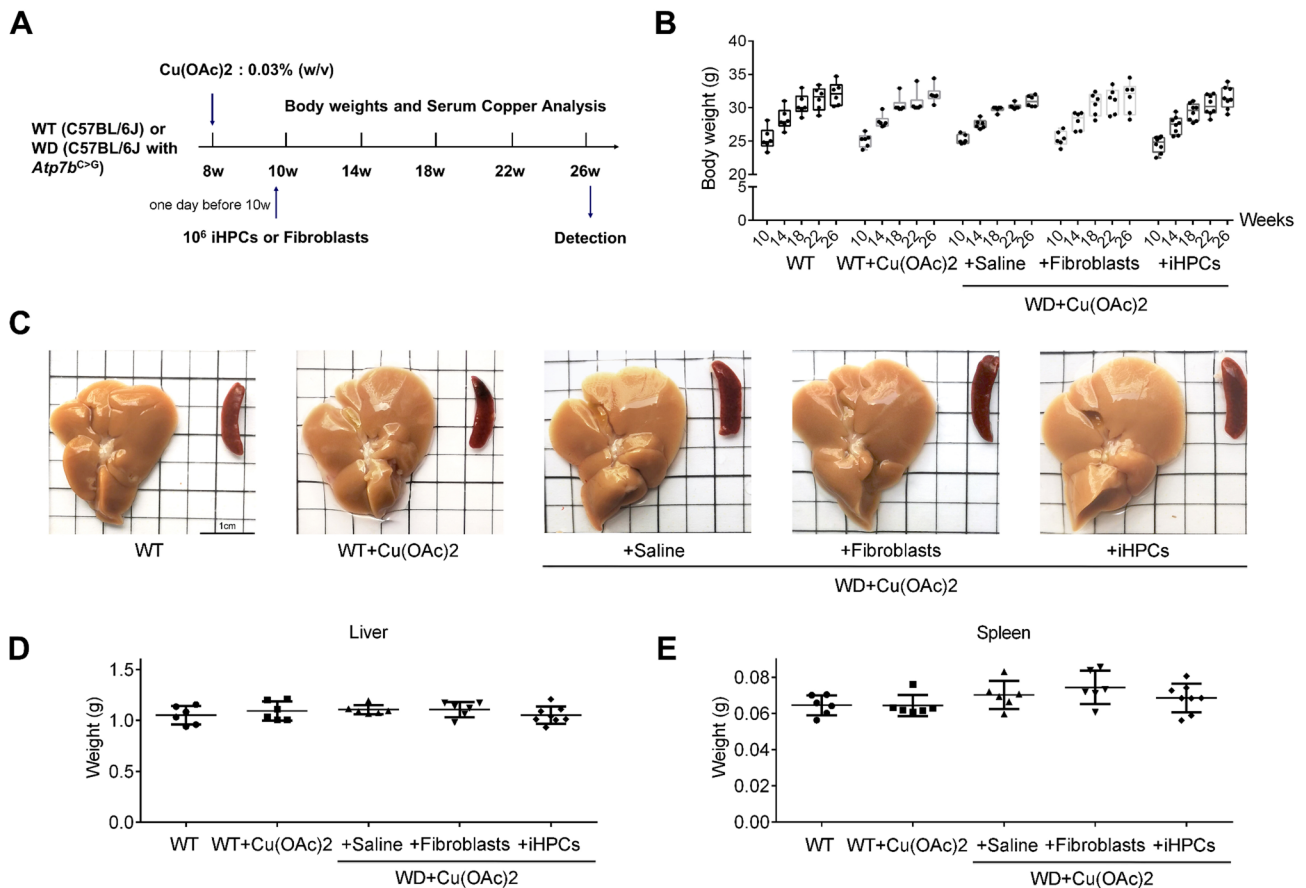
Fig. 3 Transplantation of iHPCs into the *Atp7b* (H1071Q) point mutation WD mice. **(A)** Schematic strategy of copper loading and cell transplantation of control fibroblasts and iHPCs into the WD mice. **(B)** Body weights of the mice every four weeks after cell transplantation. **(C)** Representative morphologies of livers and spleens in each group at 16 weeks post cell transplantation. Weights of the livers **(D)** and spleens **(E)** at week 16 after cell transplantation

overload (Fig. 5C). However, iHPC transplantation attenuated immune cell infiltration, extracellular matrix deposition, and copper accumulation relative to in WD mice that received fibroblast transplantation (Fig. 5C).

iHPC transplantation reduced the transcription of *Tnfα, IL-1β*, and *IL-6*, as well as the ratio of CD8⁺ T lymphocytes and natural killer cells among liver-infiltrating immune cells

To reveal the attenuation of inflammation after iHPC transplantation in WD mice, liver nonparenchymal cells were isolated and stained with multicolour antibodies. Subsequent flow cytometry analysis revealed that copper loading not only increased the ratio of dendritic cells (DCs) in WD mice but also increased the ratio of DCs in wild-type mice among liver-infiltrating CD45⁺ immune cells ($P < 0.01$, Fig. 6A). The transplantation of iHPCs into WD mice did not affect the ratio of DCs among live-infiltrating cells compared with the ratio in WD mice transplanted with control fibroblasts (Fig. 6A). However, transplantation of iHPCs into WD mice significantly reduced the ratio of CD8α⁺ T lymphocytes ($P < 0.01$, Fig. 6B) and the ratio of NK1.1⁺ natural

killer cells ($P < 0.01$, Fig. 6C) compared with those in WD mice transplanted with control fibroblasts, indicating that iHPCs attenuate inflammation by reducing the number of CD8⁺ T lymphocytes and natural killer cells. Furthermore, real-time PCR analysis revealed that transplantation of iHPCs into WD mice did not reduce the transcription of interferonγ (*Ifnγ*) and *IL-1α*, but markedly reduced the transcription of *Tnfα*, *IL-1β*, and *IL-6* compared with those in WD mice and in WD mice transplanted with control fibroblasts (Fig. 6D), suggesting that iHPC transplantation reduces liver inflammation in WD mice.

Discussion

This study provides three new findings for understanding the therapeutic effects of reprogrammed fibroblasts on WD. Simultaneous overexpression of *Foxa3* and *Hnf4α* reprogrammed fibroblasts into homogenous iHPCs. Second, these reprogrammed iHPCs could integrate into the liver tissue of WD mice without obvious transplant rejection and be retained for up to 16 weeks. Transplanted iHPCs are involved in the formation of bile canals, thus
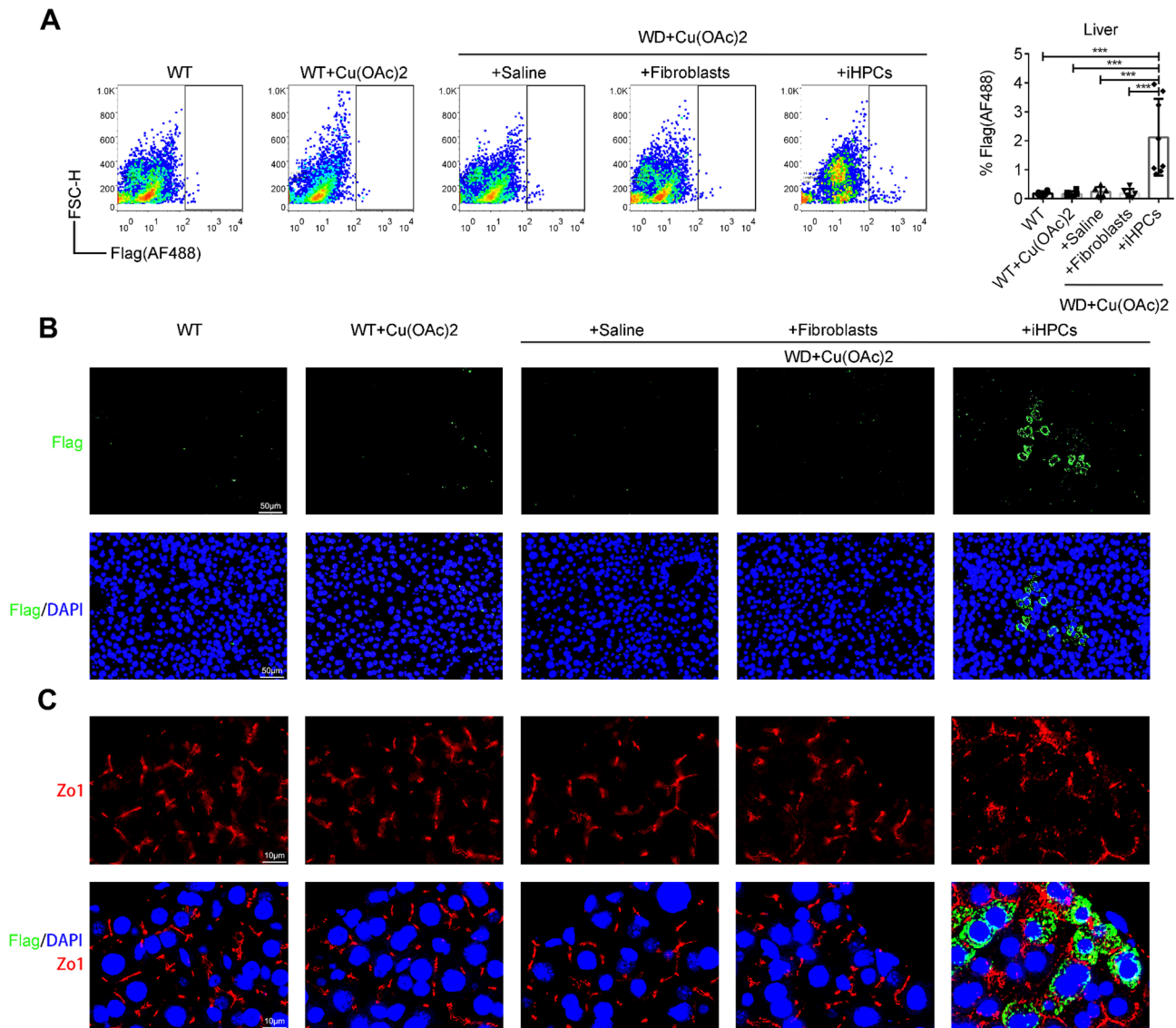
Fig. 4 iHPCs repopulated Zo1-positive hepatocytes in the livers of WD mice after transplantation. **(A)** Intracellular staining and flow cytometry analysis of the percentage of Flag-positive hepatocytes in each group. **(B)** Representative immunofluorescence images of the Flag-positive cells in liver sections from each group. Scale bars, 50 μm. **(C)** Representative images of immunofluorescence staining for Flag and Zo1 in liver sections. Scale bars, 10 μm

promoting copper secretion, reducing serum copper levels and attenuating copper accumulation-related liver disorders.

In this study, simultaneous coexpression of *Foxa3* and *Hnf4α* by lentivirus resulted in the homogeneous acquisition of new phenotypes by murine adult fibroblasts, and the reprogrammed cells could be serially passaged and successfully cryopreserved. Similar to studies that used reprogramming protocols involving multigene coexpression by multiple vectors [7–10] or multiple genes in one polycistronic vector [13–16], our method involving a single viral vector containing *Foxa3* and *Hnf4α* with their own promoters successfully draws fibroblasts out of their phenotype. However, although the gene expression profile of the cells we obtained is different from that of

fibroblasts but similar to that of liver tissues, these cells do not highly express cytochromes, as reported by other *Foxa3* plus *Hnf4α* reprogrammed mesenchymal stem cells [10, 15], but highly express Sox9, which is similar to the stem-like cells reprogrammed by *Foxa3* and *Hnf1* [11]. A possible explanation for this discrepancy may be the relatively low overexpression level of *Hnf4α*, approximately one-fourth that of *Foxa3*, which restricts reprogrammed cells to a relatively immature phenotype.

To mimic the most frequent mutation site, *ATP7B* (H1069Q), of human WD, *Atp7b* (H1071Q) point mutation WD mice were generated and used in this study. Unlike the Long-Evans Cinnamon (LEC) rat WD model, the toxic milk (TX) model, or whole *Atp7b* knockout mouse WD model [20], *Atp7b* (H1071Q) point mutation
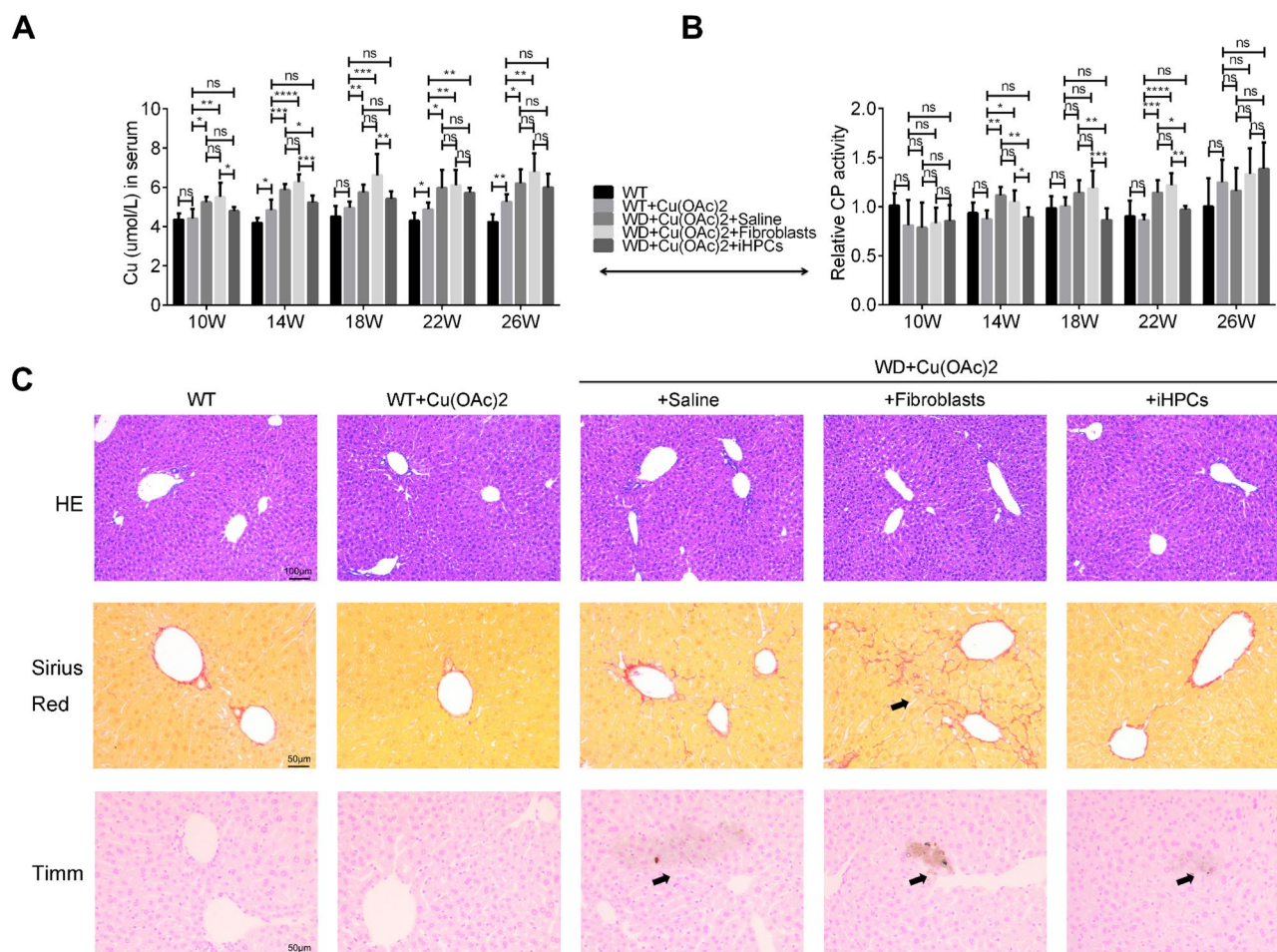
Fig. 5 Transplantation of iHPCs reduced the levels of serum copper, the relative serum ceruloplasmin activity, and the degree of collagen deposition in WD mice. The levels of serum copper **(A)** and the relative ceruloplasmin activity **(B)** in each group at 0, 4, 8, 12 and 16 weeks after cell transplantation. **(C)** Representative images of HE staining (scale bars, 100 μm), Sirius red staining (scale bars, 50 μm), and Timm's sulfide silver staining (scale bars, 50 μm) in each group

WD mice do not show any signs of liver copper accumulation under normal chow feeding. Therefore, copper acetate dissolved in the drinking water at a concentration of 0.03%, as described previously [18], was used to increase the copper loading 2 weeks before cell transplantation. Previous LEC rat studies revealed that the *Atp7b* gene could be detected *via* PCR and/or immunofluorescence staining after healthy hepatocyte transplantation [21–23]. For these *Atp7b*(H1071Q) point mutation WD mice, we used immune fluorescence staining of the Flag and flow cytometry analysis to identify the transplanted cells and to identify approximately 2% of the hepatocytes derived from iHPCs at 16 weeks posttransplantation without the ablation of native hepatocytes or the inhibition of native hepatocyte proliferation. This hepatocyte repopulation ratio is much greater than 0.04% of hepatocytes derived from bone marrow cells after 3 months of transplantation into *Atp7b*$^{-/-}$ WD mice [24], suggesting that the transplantation of fibroblast-reprogrammed

iHPCs is superior to the transplantation of bone marrow cells for WD. However, this repopulation ratio is lower than 5% of hepatocytes after transplantation of induced hepatocytes derived from gene-corrected patient-specific induced pluripotent stem cells into an immunodeficient WD mouse model (*Atp7b*$^{-/-}$/*Rag2*$^{-/-}$/*Il2rg*$^{-/-}$) for 8 weeks [25], which may be because we did not use any immunosuppressants in this study, and the weak immune rejection between the fibroblasts isolated from an inbred mouse strain C57BL/6J and the WD mice generated against the background of C57BL/6J mice may reduce the integration efficiency.

Reconstitution of the bile canal between transplanted cell-derived hepatocytes and native hepatocytes is critical for copper excretion, which is a possible reason for the ability of cell therapy to remove excess copper in WD [26]. Although we did not confirm the linear bile canaliculi between the transplanted iHPCs and their adjacent hepatocytes because of the small size of the electron
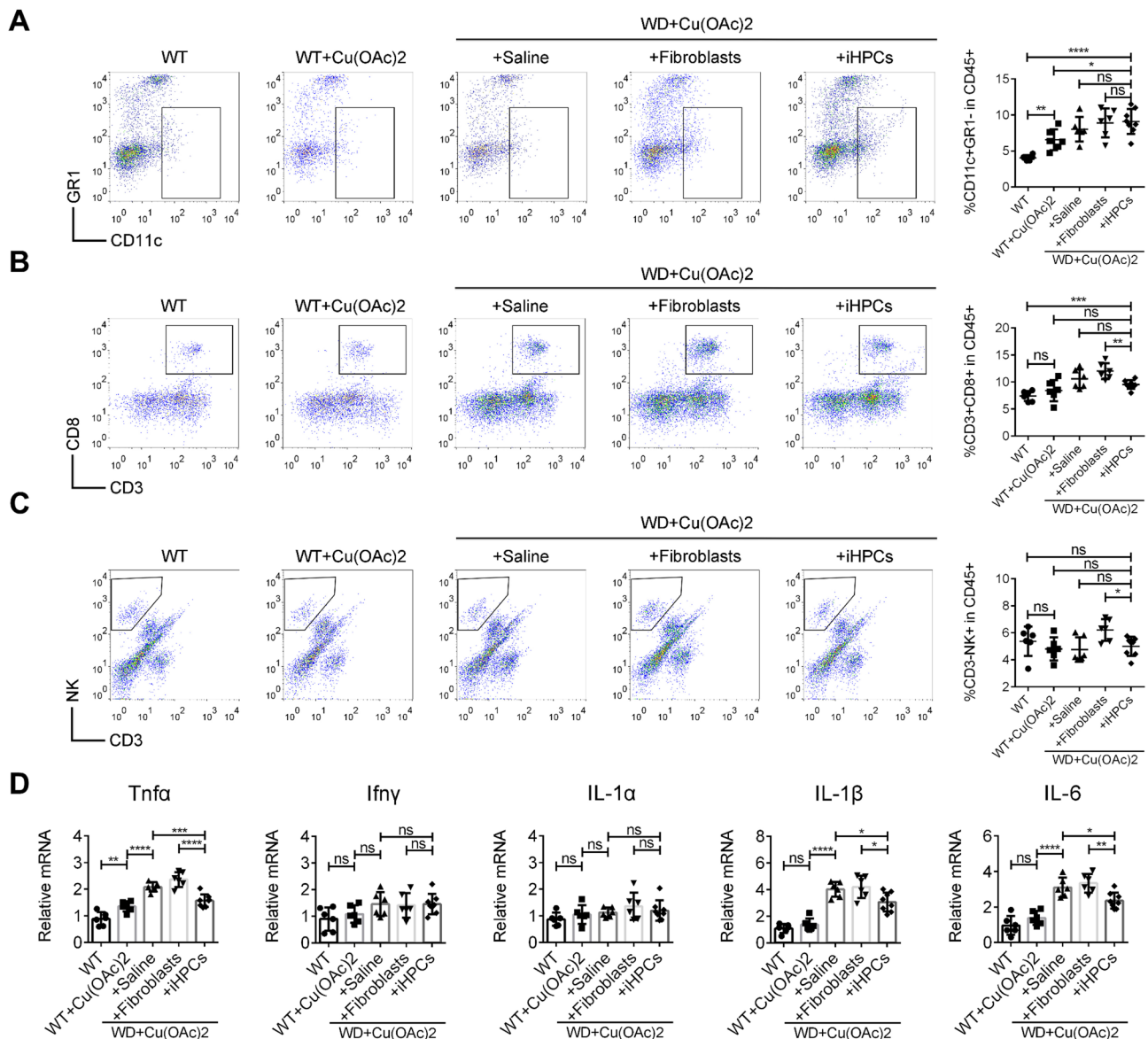
Fig. 6 Transplantation of iHPCs downregulated the transcription of inflammatory cytokines and reduced the percentages of CD8+ T lymphocytes and natural killer cells among nonparenchymal cells in WD mice. Representative flow cytometry data and statistical analysis of the percentages of CD11c+GR1− dendritic cells (**A**), CD3+CD8+ T lymphocytes (**B**), and CD3−NK1.1+ natural killer cells (**C**) among liver-infiltrating CD45+ immune cells. (**D**) Real-time PCR analysis revealed the relative transcription levels of *Tnfa*, *Ifnγ*, *IL-1a*, *IL-1β*, and *IL-6* in the liver

microscope sample and the low percentage of integrated cells (2%) among the whole liver tissue by immunoelectron microscopy, the iHPC-derived hepatocytes expressed the tight junction-associated protein Zo1, an essential compartment for bile canaliculi [27, 28], after reprogramming and continuing to express Zo1 among the recipient hepatocytes, suggesting possible bile canalicular formation between the transplanted cells and the recipient hepatocytes. Therefore, iHPC transplantation reduces liver copper deposition and serum copper levels, thereby attenuating the transcription of the proinflammatory cytokines and reducing the infiltration of CD8+

T lymphocytes and natural killer cells to promote therapeutic effects on WD. We also noted that the reduction in serum copper and ceruloplasmin levels was marked at 8 weeks posttransplantation but was not significantly different at 16 weeks posttransplantation. This may be due to copper loading-induced disease progression and the number of transplanted iHPC-derived hepatocytes being insufficient for copper excretion.

Conclusions

In summary, the coexpressing of Foxa3 and Hnf4α effectively reprograms fibroblasts into hepatic progenitor cells. These induced hepatic progenitor cells are capable of integrating into liver tissue, forming tight junction amidst the native hepatocytes, reducing serum copper levels, and attenuating copper accumulation-related liver disorders, thus providing a new therapeutic strategy for WD.

Abbreviations

iHPCs	Induced hepatic progenitor cells
WD	Wilson's disease
WT	Wild-type
Cu	Copper
CP	Ceruloplasmin
HE	Haematoxylin and eosin
DCs	Dendritic cells
TX	Toxic milk
PAS	Periodic acid Schiff

Supplementary Information

The online version contains supplementary material available at https://doi.org/10.1186/s13287-025-04253-1.

> Supplementary Table 1
>
> Supplementary Material 2

Author contributions

Credit author statement: KL performed the cell culture studies and animal studies, designed and performed experiments, analysed the data, wrote the manuscript, produced figures and acquired funding. LL, YH, and SZ helped to perform the animal experiments, collected data and provided discussion. HY designed experiments, analysed data and provided discussion. PW designed experiments, supervised the study, analysed data, revised the manuscript and acquired funding. All the authors have read the manuscript, provided critical comments, and approved the final version of this manuscript.

Data availability

The RNA sequencing data (Genome Sequence Archive with the accession number CRA010018) used during the study are available online in accordance with funder data-retention policies.

Declarations

Ethics approval and consent to participate

All experiments involving animals were conducted according to ethical policies and procedures approved by the Ethics Committee of the Beijing Friendship Hospital, Capital Medical University, China (Approval No. 21-2051). The title of the approved project is "Study on the Mechanism of iHPCs Therapy in Wilson's Disease." The approval date is December 30, 2021.

Consent for publication

Not applicable.

Conflict of interest

The authors declare that they have no competing interests.

Author details

¹Beijing Key Laboratory of Tolerance Induction and Organ Protection in Transplantation, Beijing Friendship Hospital, Capital Medical University, No. 95 Yong An Road, Beijing 100050, China
²Beijing Clinical Research Institute, Beijing 100050, China
³Liver Research Center, Beijing Friendship Hospital, Capital Medical University, Beijing 100050, China
⁴National Clinical Research Center for Digestive Disease, Beijing 100069, China

References

1. Członkowska A, Litwin T, Dusek P, Ferenci P, Lutsenko S, Medici V, Rybakowski JK, Weiss KH, Schilsky ML. Wilson disease. Nat Rev Dis Primers. 2018;4(1):21.
2. Mulligan C, Bronstein JM. Wilson disease: an overview and approach to management. Neurol Clin. 2020;38(2):417–32.
3. Litwin T, Dzieżyc K, Członkowska A. Wilson disease-treatment perspectives. Ann Transl Med. 2019;7(Suppl 2):S68.
4. Ahmad A, Torrazza-Perez E, Michael L, Schilsky ML. Liver transplantation for Wilson disease. Handb Clin Neurol. 2017;142:193–204.
5. Park SM, Kim Vo K, Lallier M, Cloutier AS, Brochu P, Alvarez F, Martin SR. Hepatocyte transplantation in the long Evans cinnamon rat model of Wilson's disease. Cell Transpl. 2006;15(1):13–22.
6. Sauer V, Siaj R, Stöppeler S, Bahde R, Spiegel HU, Köhler G, Zibert A, Schmidt HHJ. Repeated transplantation of hepatocytes prevents fulminant hepatitis in a rat model of Wilson's disease. Liver Transpl. 2012;18(2):248–59.
7. Huang P, He Z, Ji S, Sun H, Xiang D, Liu C, Hu Y, Wang X, Hui L. Induction of functional hepatocyte-like cells from mouse fibroblasts by defined factors. Nature. 2011;475(7356):386–9.
8. Sekiya S, Suzuki A. Direct conversion of mouse fibroblasts to hepatocyte-like cells by defined factors. Nature. 2011;475(7356):390–3.
9. Huang P, Zhang L, Gao Y, He Z, Yao D, Wu Z, Cen J, Chen X, Liu C, Hu Y, Lai D, Hu Z, Chen L, Zhang Y, Cheng X, Ma X, Pan G, Wang X, Hui L. Direct reprogramming of human fibroblasts to functional and expandable hepatocytes. Cell Stem Cell. 2014;14(3):370–84.
10. Dai K, Chen R, Ding Y, Niu Z, Fan J, Xu C. Induction of functional Hepatocyte-Like cells by overexpression of FOXA3 and HNF4α in rat bone marrow mesenchymal stem cells. Cells Tissues Organs. 2014;200(2):132–40.
11. Yu B, He ZY, You P, Han QW, Xiang D, Chen F, Wang MJ, Liu CC, Lin XW, Borjigin U, Zi XY, Li JX, Zhu HY, Li WL, Han CS, Wangensteen KJ, Shi Y, Hui LJ, Wang X, Hu YP. Reprogramming fibroblasts into bipotential hepatic stem cells by defined factors. Cell Stem Cell. 2013;13(3):328–40.
12. Rombaut M, Boeckmans J, Rodrigues RM, van Grunsven LA, Vanhaecke T, Kock JD. Direct reprogramming of somatic cells into induced hepatocytes: cracking the enigma code. J Hepatol. 2021;75(3):690–705.
13. Chen C, Pla-Palacín I, Baptista PM, Shang P, Oosterhoff LA, van Wolferen ME, Penning LC, Geijsen N, Spee B. Hepatocyte-like cells generated by direct reprogramming from murine somatic cells can repopulate decellularized livers. Biotechnol Bioeng. 2018;115(11):2807–16.
14. Song G, Pacher M, Balakrishnan A, Yuan Q, Tsay HC, Yang D, Reetz J, Brandes S, Dai Z, Pützer BM, Araúzo-Bravo MJ, Steinemann D, Luedde T, Schwabe RF, Manns MP, Schöler HR, Schambach A, Cantz T, Ott M, Sharma AD. Direct reprogramming of hepatic myofibroblasts into hepatocytes in vivo attenuates liver fibrosis. Cell Stem Cell. 2016;18(6):797–808.
15. Katayama H, Yasuchika K, Miyauchi Y, Kojima H, Yamaoka R, Kawai T, Yoshitoshi EY, Ogiso S, Kita S, Yasuda K, Sasaki N, Fukumitsu K, Komori J, Ishii T, Uemoto S. Generation of non-viral, transgene-free hepatocyte like cells with piggybac transposon. Sci Rep. 2017;7:44498.
16. Ballester M, Bolonio M, Santamaria R, Castell JV, Ribes-Koninckx C, Bort R. Direct conversion of human fibroblast to hepatocytes using a single inducible polycistronic vector. Stem Cell Res Ther. 2019;10(1):317.
17. Liu Z, Chen O, Wall JBJ, Zheng M, Zhou Y, Wang L, Vaseghi HR, Qian L, Liu J. Systematic comparison of 2A peptides for cloning multi-genes in a polycistronic vector. Sci Rep. 2017;7(1):2193.

18. Allen KJ, Cheah DMY, Lee XL, Pettigrew-Buck NE, Vadolas J, Mercer JFB, Ioannou PA, Williamson R. The potential of bone marrow stem cells to correct liver dysfunction in a mouse model of Wilson's disease. Cell Transpl. 2004;13(7–8):765–73.

19. Wang P, Zhang H, Li W, Zhao Y, An W. Promoter-defined isolation and identification of hepatic progenitor cells from the human fetal liver. Histochem Cell Biol. 2008;130:375–85.

20. Medici V, Dominik Huster D. Animal models of Wilson disease. Handb Clin Neurol. 2017;142:57–70.

21. Malhi H, Irani AN, Volenberg I, Schilsky ML, Gupta S. Early cell transplantation in LEC rats modeling Wilson's disease eliminates hepatic copper with reversal of liver disease. Gastroenterology. 2002;122(2):438–47.

22. Irani AN, Malhi H, Slehria S, Gorla GR, Volenberg I, Schilsky ML, Gupta S. Correction of liver disease following transplantation of normal rat hepatocytes into Long-Evans cinnamon rats modeling Wilson's disease. Mol Ther. 2001;3(3):302–9.

23. Park SM, Vo K, Lallier M, Cloutier AS, Brochu P, Alvarez F, Martin SR. Hepatocyte transplantation in the long Evans cinnamon rat model of Wilson's disease. Cell Transpl. 2006;15(1):13–22.

24. Sharma Y, Liu J, Kristian KE, Follenzi A, Gupta S. In Atp7b-/- mice modeling Wilson's disease liver repopulation with bone Marrow-Derived myofibroblasts or inflammatory cells and not hepatocytes is deleterious. Gene Expr. 2018;19(1):15–24.

25. Wei R, Yang J, Cheng CW, Ho WI, Li N, Hu Y, Hong X, Fu J, Yang B, Liu Y, Jiang L, Lai WH, Au KW, Tsang WL, Tse YL, Ng KM, Esteban MA, Tse HF. CRISPR-targeted genome editing of human induced pluripotent stem cell-derived hepatocytes for the treatment of Wilson's disease. JHEP Rep. 2021;4(1):100389.

26. Gupta S. Cell therapy to remove excess copper in Wilson's disease. Ann N Y Acad Sci. 2014;1315(1):70–80.

27. Depreter M, Walker T, De Smet K, Beken S, Kerckaert I, Rogiers V, Roels F. Hepatocyte Polarity and the peroxisomal compartment: a comparative study. Histochem J. 2002;34(3–4):139–51.

28. Rao RK, Samak G. Bile duct epithelial tight junctions and barrier function. Tissue Barriers. 2013;1(4):e25718.

Publisher's note

Springer Nature remains neutral with regard to jurisdictional claims in published maps and institutional affiliations.